Glueballs at Finite Temperature in Lattice QCD

J.B. Zhang
Institute of Modern Physics,
Zhejiang Univ. Hangzhou, China
Collaborators:
Y.Chen, G. Li, C. Liu, Y.B. Liu,
J.P. Ma, X.F.Meng.

Tony Thomas's 60th Birthday Fest
Feb. 15-19, 2010, Adelaide

Outline

I. Motivation

II. Numerical details

III. Glueballs at finite temperature

  a) Cosh-function fit

  b) Breit-Wigner ansatz

IV. Summary

I. Motivation

- The QGP at the RHIC experiments is most likely a strongly interacting system.

The data of RHIC experiments are well described by the ideal hydrodynamic model

The investigation of elliptic flow data using a Boltzmann-type equation for gluon scattering are not consistent with the pQCD.

- # Meson correlators at finite temperature

$$C(\tau,T)=\int_0^{\infty} d\omega\rho(\omega,T)K(\tau,\omega,T), \quad K(\tau,\omega,T)=\frac{\cosh(\omega(\tau-1/2T))}{2\sinh(\omega/2T)}$$

1. **Charmonia** (S. Datta et al, Phys. Rev. D 69 (2004) 094507)

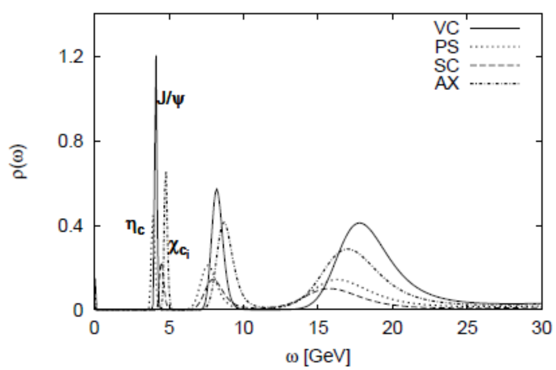

$T < T_c$

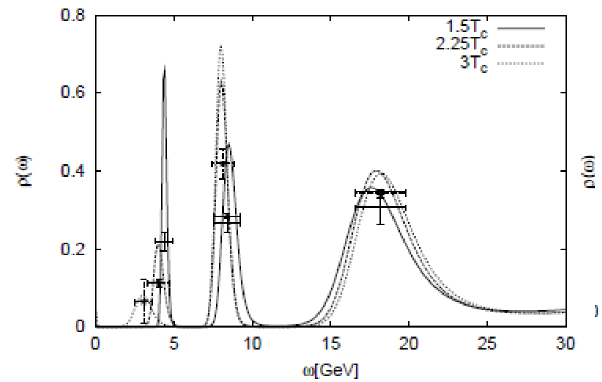

$J/\psi(T > T_c)$

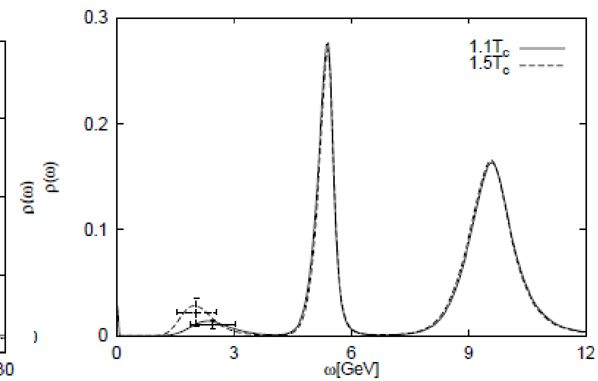

$\chi_{c0}(T > T_c)$

- 1S charmonia survive up to temperature $T \sim 2.25T_c$
- The spectral function implies a gradual dissolution.*
- 1P charmonia dessolve at $T \sim 1.1T_c$

• Another early study found an abrupt disapperance of 1S states at $T \sim 1.7 T_c$

(M. Asakawa and T. Hatsuda, Phys. Rev. Lett. 92 (2004) 012001)

• A more recent study

Charmonium at high temperature in two-flavor QCD

Gert Aarts, Chris Allton,Mehmet Bugˇrahan Oktay, Mike Peardon, and Jon-Ivar Skullerud

(Phys. Rev. D. 76 (2007) 094513)

S-waves (J/ψ and η_c) survive up to temperatures close to $2T_c$, while the P-waves (χ_{c0} and χ_{c1}) melt away below $1.2T_c$.

2. Light hadrons

(M. Asakawa et al,
Nucl. Phys. A 715 (2003) 863)

- The spectral functions of light hadrons abovt Tc don't show continuum-like structure that can be identified as free quarks but peaks.

- The behaviors of the spectral function meet the common expectation that the pseudo-scalar and scalar correlators degenerate at high temperature due to the restoration of chiral symmetry.

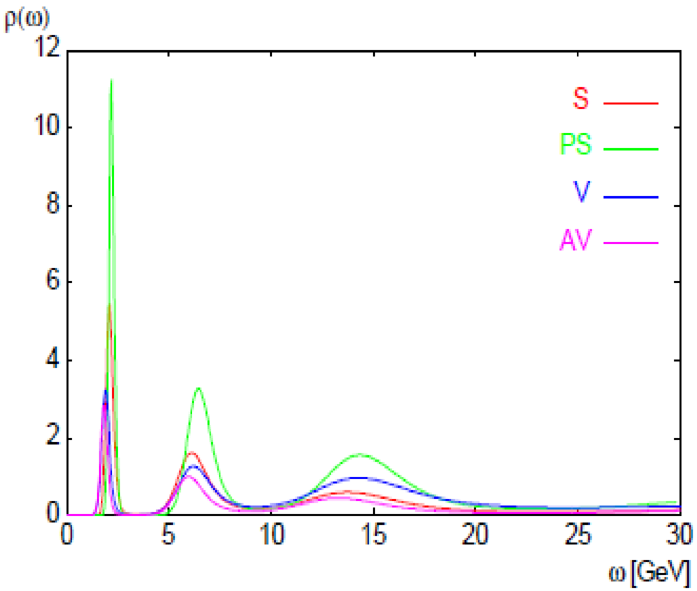

Spectral functions above deconfinement for

$$m_{PS} / m_V \approx 0.65$$

i.e, for quark masses around the strange quark mass.

3. **Glueballs** ?????

- Gluon bound states predict by QCD
- Well defined in pure gauge theory
- Their properties below and above the deconfinement phase transition is desired.

II. Numerical details

1. Lattices and the gauge action

- Anisotropic lattices with the temporal lattice spacing much smaller than the spatial one.
- The tadpole improved Symanzik's action

$$S_{IA} = \beta\{\frac{5}{3}\frac{\Omega_{sp}}{\xi u_s^4} + \frac{4}{3}\frac{\xi\Omega_{tp}}{u_t^2 u_s^2} - \frac{1}{12}\frac{\Omega_{sr}}{\xi u_s^6} - \frac{1}{12}\frac{\xi\Omega_{str}}{u_s^4 u_t^2}\}$$

$$\Omega_C = \sum_C \tfrac{1}{3} ReTr(1 - W_C)$$

$$u_s = < \tfrac{1}{3} TrP_{ss'} >^{1/4} \qquad u_t = 1$$

$$\xi = a_s/a_t$$

($\xi = 5$ in this work)

2. Glueball operators

• Symmetry group and corresponding quantum numbers on the lattice

	Continuum	Cubic lattice
Symmetry group	$SO(3)\otimes P\otimes C$	$O\otimes P\otimes C$
Irreducible representations	J^{PC} $J=0,1,2,\ldots$ $PC=++,+-,-+,--$	R^{PC} $R=A_1,A_2,E,T_1,T_2$ $PC=++,+-,-+,--$

Building prototypes
(various Wilson loops)

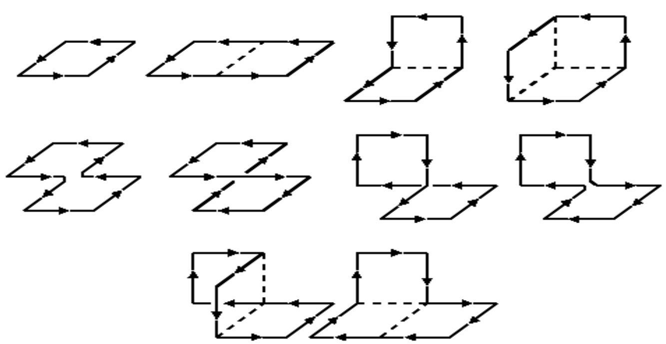

- **Smearing Schemes**

Single link smearing (APE smearing)

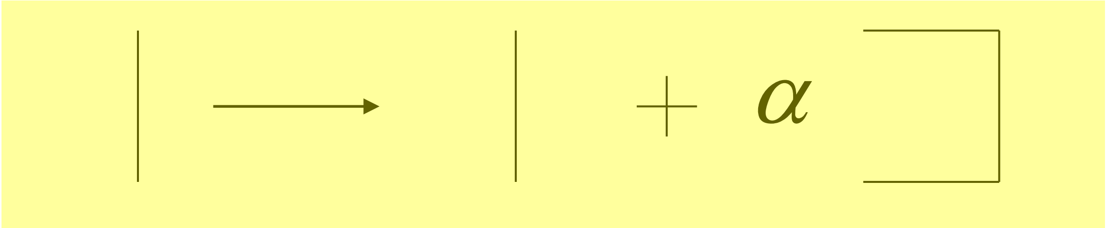

Double link smearing (fuzzying)

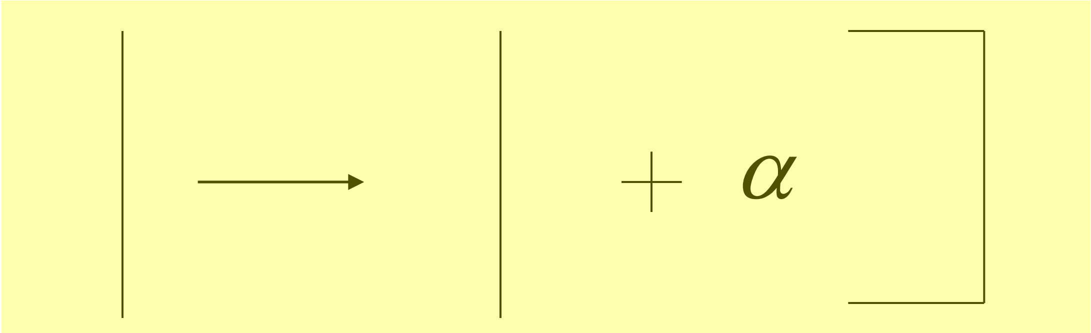

Combining the 6 smearing schemes of gauge links and different 4 prototypes of Wilson loops mentioned above, we have a set of 24 different operators for each R^{PC}

$$\{\phi_\alpha, \alpha = 1,2,\ldots,24\}$$

- **Variational method** (VM)

The essence of the VM is to find a set of combinational coefficients

$$\{v_\alpha, \alpha = 1,2,\ldots 24\}$$

such that the operator

$$\Phi = \sum_\alpha v_\alpha \phi_\alpha$$

couples mostly to a specific state.

This can be realized by solving the generalized eigenvalue problem

$$\tilde{C}(t_D)\mathbf{v}^{(R)} = e^{-t_D \tilde{m}(t_D)} \tilde{C}(0)\mathbf{v}^{(R)}$$

$$\tilde{C}_{\alpha\beta}(t) = \sum_\tau \langle 0|\phi_\alpha(t+\tau)\phi_\beta(\tau)|0\rangle$$

$$\tilde{m}(t_D) = -\frac{1}{t_D} \ln \frac{\sum_{\alpha\beta} v_\alpha v_\beta \tilde{C}_{\alpha\beta}(t_D)}{\sum_{\alpha\beta} v_\alpha v_\beta \tilde{C}_{\alpha\beta}(0)}$$

3. The deconfinement critical point

On the lattice the temperature is defined as

$$T = \frac{1}{N_t a_t}$$

There are two ways to vary the temperature:

1) change the temporal lattice size;

2) change the lattice spacing

$$a = \frac{1}{\Lambda} f(g) \qquad g \leftrightarrow \beta$$

Since the bare coupling constant g can be varied continuously, we first determine the critical coupling constant for a fixed temporal lattice size $N_t = 24$

The order parameter $\chi_P = \langle \Theta^2 \rangle - \langle \Theta \rangle^2$

on 24^4 lattice
after a β scan,
the critical point is
around $\beta \approx 2.81$

$$\Theta = \begin{cases} \mathrm{Re} P \exp[-2\pi i/3]; & \arg P \in [\pi/3, \pi) \\ \mathrm{Re} P; & \arg P \in [-\pi/3, \pi/3) \\ \mathrm{Re} P \exp[2\pi i/3]; & \arg P \in [-\pi, -\pi/3) \end{cases}$$

Spectral density method:

After the extrapolation,
the peak position gives
the critical point,

$$\beta_c = 2.808$$

With the lattice spacing

$$r_0 / a_s = 3.476,$$

$$T_c = 0.724 r_0^{-1} \approx 296 MeV$$

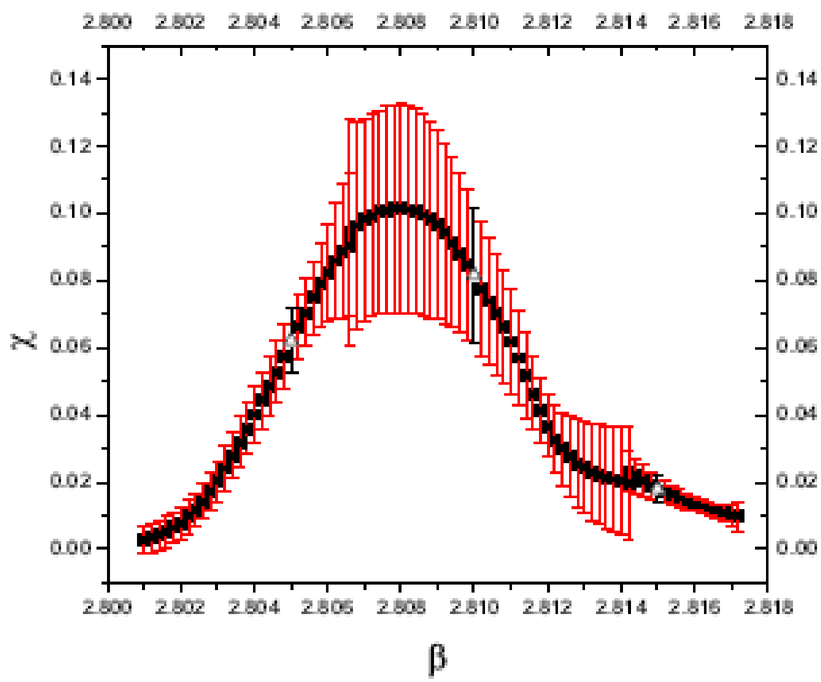

Determination of working β

- First, the spatial volume is large enough in order for glueballs to be free of sizable finite volume effects.
- Secondly, the temporal lattice has good resolution even at $T \sim 2T_c$

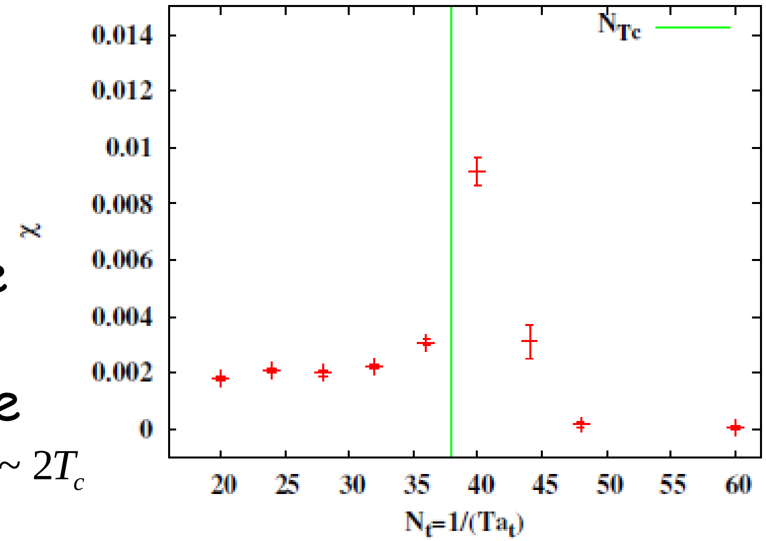

$$\beta = 3.2 \qquad N_s^3 \times N_t = 24^3 \times 128$$

$$V(r) = V_0 + \sigma r + \frac{e_c}{r}$$

$$\frac{a_s}{r_0} = \sqrt{\frac{\sigma a_s^2}{1.65 + e_c}} = 0.1825(7)$$

$$a_s = 0.0878(4)\,\mathrm{fm}$$

$$T_c : N_t \sim 39$$

$$2T_c : N_t \sim 20$$

TABLE III: Simulation parameters to calculate glueball spectrum. $\beta = 3.2$, $a_s = 0.0878$ fm, $L_s = 2.11$ fm.

N_t	T/T_c	n_{mb}	N_{bin}
128	0.30	80	120
80	0.47	80	150
60	0.63	80	220
48	0.79	80	200
44	0.86	80	220
40	0.95	80	200
36	1.05	80	200
32	1.19	80	280
28	1.36	80	200
24	1.58	80	200
20	1.90	80	200

III. Glueballs at finite temperature

1. The glueball spectrum at T=0

The latest glueball spectrum from quenched LQCD
(Y. Chen et al, Phys. Rev. D 73, 014516 (2006)

J^{PC}	$r_0 M_G$	M_G (MeV)
0^{++}	4.16(11)(4)	1710(50)(80)
2^{++}	5.83(5)(6)	2390(30)(120)
0^{-+}	6.25(6)(6)	2560(35)(120)
1^{+-}	7.27(4)(7)	2980(30)(140)
2^{-+}	7.42(7)(7)	3040(40)(150)
3^{+-}	8.79(3)(9)	3600(40)(170)
3^{++}	8.94(6)(9)	3670(50)(180)
1^{--}	9.34(4)(9)	3830(40)(190)
2^{--}	9.77(4)(10)	4010(45)(200)
3^{--}	10.25(4))(10)	4200(45)(200)
2^{+-}	10.32(7)(10)	4230(50)(200)
0^{+-}	11.66(7)(12)	4780(60)(230)

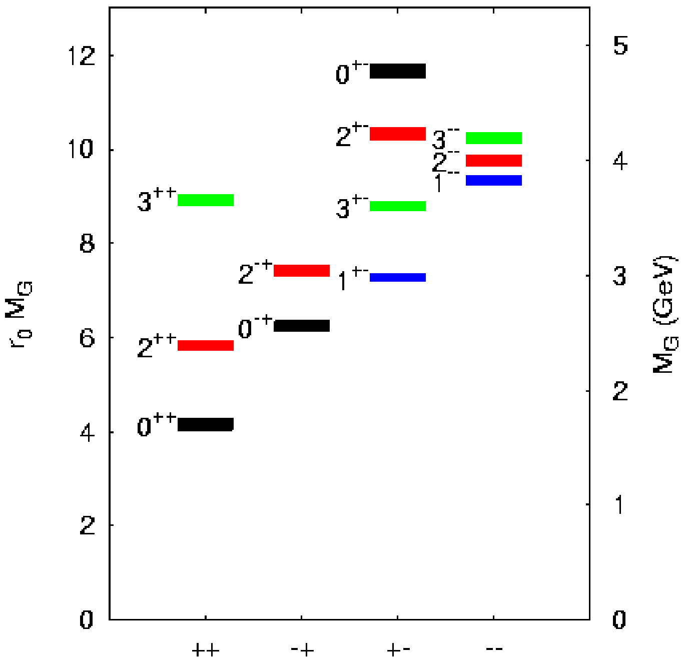

2. The glueball correlators

In the spectral representation

$$C(t,T) \equiv \frac{1}{Z(T)}\mathrm{Tr}\left(e^{-H/T}\Phi(t)\Phi(0)\right) = \int_{-\infty}^{\infty} d\omega\rho(\omega)K(\omega,T),$$

$$\rho(\omega) = \sum_{m,n}\frac{|\langle n|\Phi|m\rangle|^2}{2Z(T)}e^{-E_m/T} \times (\delta(\omega-(E_n-E_m)-\delta(\omega-(E_m-E_n))$$

In the T=0 case, the spectral function reduces to

$$\rho(\omega) = \sum_n \frac{|\langle 0|\Phi|n\rangle|^2}{2Z(0)}(\delta(\omega-E_n)-\delta(\omega+E_n))$$

Thus, we have the conventional function form of correlators

$$C(t,T=0) = \sum_n W_n e^{-E_n\tau}$$

For finite temperature $T \neq 0$

$$\rho(\omega) = \sum_{m,n} \frac{|\langle n|\Phi|m\rangle|^2}{2Z(T)} e^{-E_m/T} \times (\delta(\omega - (E_n - E_m) - \delta(\omega - (E_m - E_n))$$

all the thermal states $|m\rangle$ with non-vanishing matrix elements $\langle m|\Phi|n\rangle \neq 0$ contribute to the spectral function. The contribution is weighted by the factor

$$\exp\left(-\frac{E_m}{T}\right)$$

For the pure SU(3) gauge theory, since in the confinement phase the thermal degrees of freedom are hadron-like modes (glueballs), apart from the vacuum, the maximal value of this factor is

$$\exp\left(-\frac{M}{T}\right)$$

where M is the mass of the lightest glueball. In the scalar channel with M~1.6 GeV, this factor at T=T_c is estimated to be 0.003, which is much smaller than 1. Therefore the spectral function at 0<T<T_c is almost the same as T=0 case.

a. The single-cosh fit

Pole mass

$$C(t,T)=\sum_n W_n \frac{\cosh(M_n(1/(2T)-t))}{\sinh(M_n/(2T))},$$

Based on the discussion above, we would like to use this function form to analyze the glueball correlators all over the temperature in concern:

- the thermal scattering of the glueball-like modes would result in a mass shift, say, the deviation of the pole mass from the zero-temperature glueball mass, which reflects the strength of the interaction at different temperature.

- the breakdown of this function form would signal the dominance of new degrees of freedom.

Effective mass plateaus

A_1^{++}

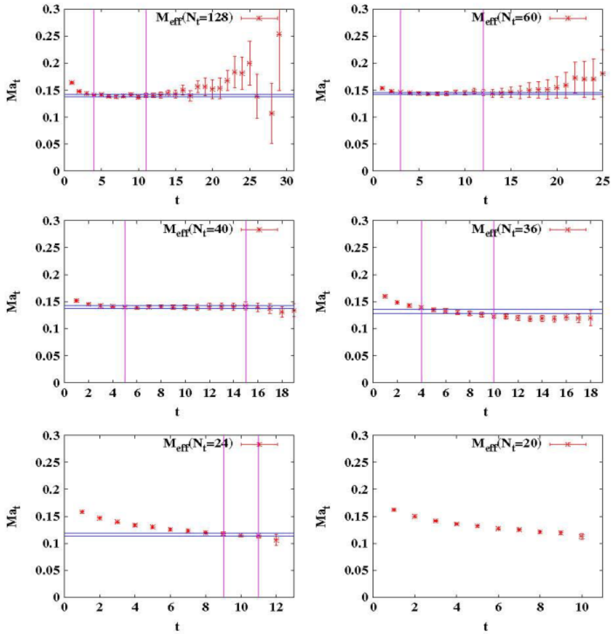

A_1^{-+}

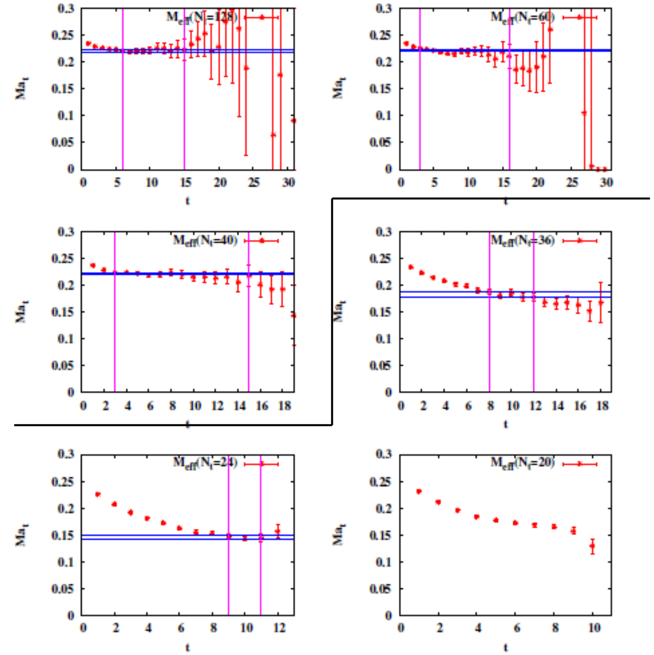

E^{++}

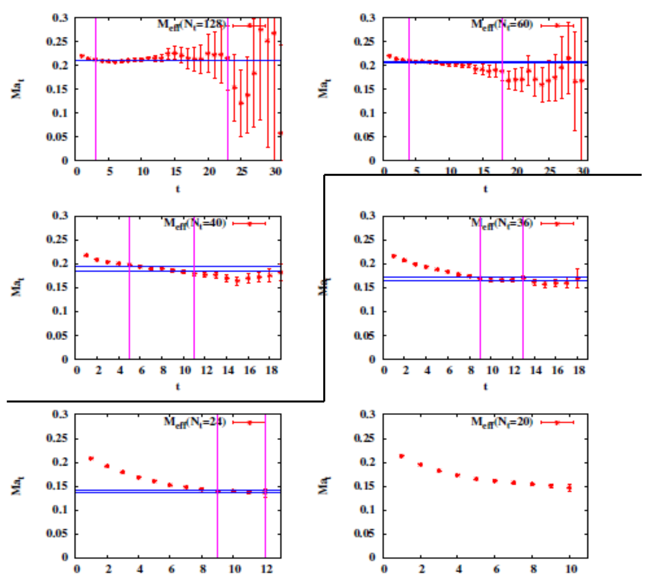

T_2^{++}

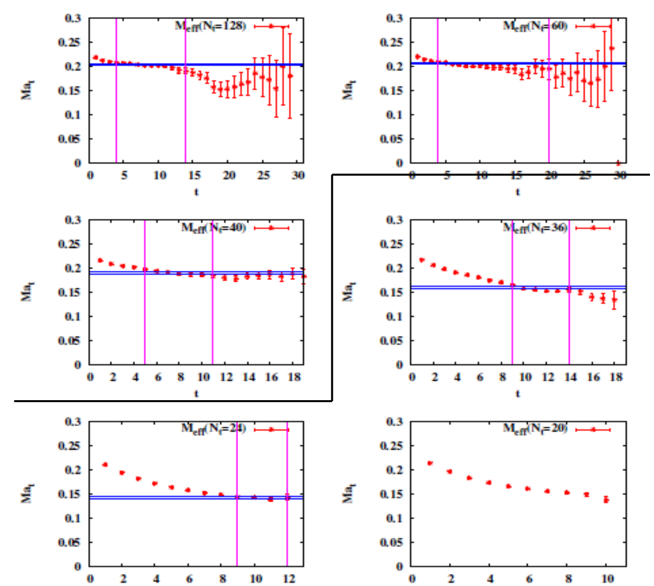

The pole masses glueballs in all the 20 symmetry channels

TABLE IV: The pole masses in all the 20 R^{PC} channels are extracted at all the temperatures. The mass values are in units of a_t^{-1}.

R^{PC}	128	80	60	48	44	40	36	32	28	24
A_1^{++}	0.150(1)	0.152(2)	0.154(1)	0.160(2)	0.156(2)	0.159(2)	0.144(4)	0.132(2)	0.126(3)	0.120(3)
A_1^{+-}	0.441(3)	0.435(3)	0.434(5)	0.437(4)	0.432(4)	0.435(5)	0.399(6)	0.322(9)	0.267(16)	0.241(13)
A_1^{-+}	0.221(3)	0.225(2)	0.222(2)	0.225(2)	0.218(3)	0.222(2)	0.183(5)	0.174(3)	0.155(4)	0.146(4)
A_1^{--}	0.475(6)	0.453(8)	0.447(9)	0.464(7)	0.473(6)	0.468(6)	0.426(12)	0.417(10)	0.287(19)	0.253(18)
A_2^{++}	0.323(4)	0.327(4)	0.326(4)	0.330(2)	0.326(4)	0.332(3)	0.282(7)	0.249(8)	0.224(9)	0.208(9)
A_2^{+-}	0.302(5)	0.308(3)	0.308(5)	0.312(3)	0.312(5)	0.308(6)	0.268(6)	0.241(7)	0.220(8)	0.201(6)
A_2^{-+}	0.450(5)	0.449(7)	0.446(5)	0.440(6)	0.452(4)	0.448(5)	0.396(10)	0.340(11)	0.330(12)	0.250(14)
A_2^{--}	0.387(3)	0.388(3)	0.385(4)	0.390(5)	0.376(4)	0.375(4)	0.354(7)	0.293(7)	0.268(10)	0.214(9)
E^{++}	0.210(1)	0.205(1)	0.207(1)	0.209(2)	0.206(1)	0.189(4)	0.167(4)	0.153(3)	0.143(3)	0.139(2)
E^{+-}	0.401(2)	0.403(2)	0.401(2)	0.394(4)	0.400(2)	0.395(3)	0.375(4)	0.311(6)	0.261(7)	0.230(7)
E^{-+}	0.273(1)	0.266(1)	0.264(2)	0.273(2)	0.275(1)	0.262(2)	0.218(4)	0.196(4)	0.183(4)	0.181(4)
E^{--}	0.374(1)	0.368(2)	0.360(2)	0.361(3)	0.363(3)	0.352(4)	0.308(8)	0.262(6)	0.231(6)	0.213(6)
T_1^{++}	0.327(2)	0.326(4)	0.327(2)	0.334(2)	0.331(2)	0.312(5)	0.287(7)	0.266(3)	0.227(6)	0.215(4)
T_1^{+-}	0.278(1)	0.274(2)	0.265(3)	0.278(2)	0.281(1)	0.261(3)	0.207(6)	0.199(2)	0.181(4)	0.175(2)
T_1^{-+}	0.372(2)	0.377(4)	0.371(3)	0.380(2)	0.374(2)	0.370(3)	0.331(5)	0.289(7)	0.248(7)	0.230(5)
T_1^{--}	0.350(4)	0.349(2)	0.344(3)	0.351(2)	0.350(2)	0.343(3)	0.272(8)	0.252(5)	0.212(6)	0.201(5)
T_2^{++}	0.205(1)	0.209(1)	0.206(1)	0.205(1)	0.207(2)	0.191(3)	0.160(3)	0.152(2)	0.148(2)	0.143(2)
T_1^{+-}	0.322(2)	0.317(2)	0.310(4)	0.317(3)	0.320(2)	0.303(5)	0.276(5)	0.250(3)	0.201(4)	0.190(4)
T_1^{-+}	0.265(2)	0.260(3)	0.264(2)	0.273(3)	0.272(2)	0.264(2)	0.240(3)	0.213(3)	0.187(4)	0.183(4)
T_1^{--}	0.368(2)	0.358(3)	0.364(3)	0.358(4)	0.367(2)	0.353(5)	0.282(13)	0.254(6)	0.235(6)	0.220(4)

T_c

Information inferred from the single-cosh analysis

- Below T_c, the thermal correlators of glueballs can be well described by the single-cosh function form, and the pole masses are stable with the varying T;
- Glueball-like modes survive up to 1.6T_c in the deconfinement phase.
- The pole masses decrease gradually above T_c.
- These observations apply to all the 20 symmetry channels.

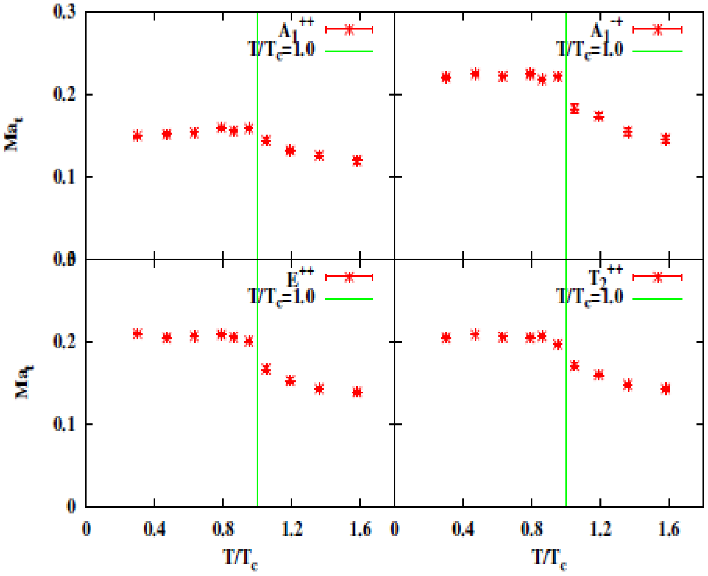

The figure illustrates the behaviors of glueball masses with respect to the varying temperature.

However, our results are different from those of a previous work

(N. Ishii et al, Phys. Rev. D 66, 094506 (2002))

0^{++}

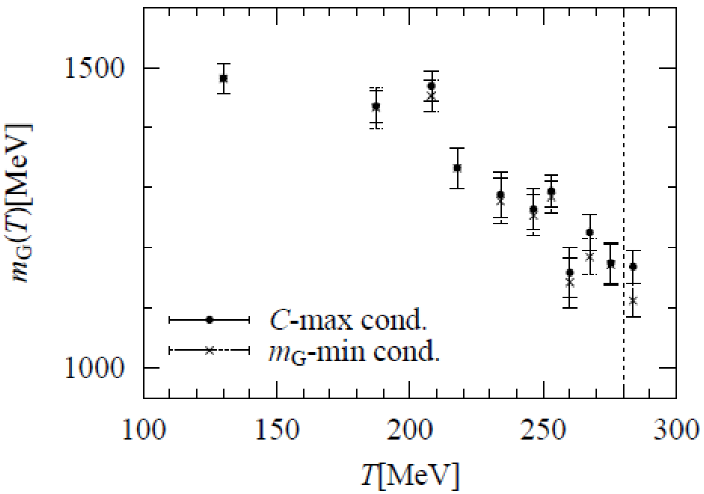

2^{++}

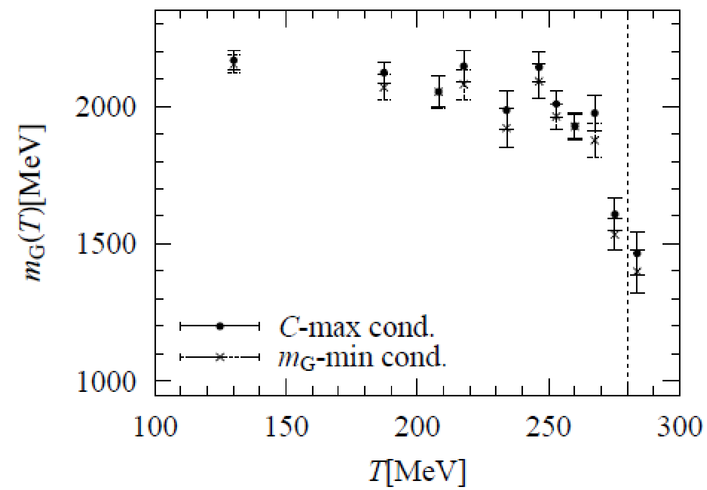

$$m_G(T \sim 0) - m_G(T \simeq T_c) \simeq 300\mathrm{MeV},$$

$$m_G(T \simeq T_c) \simeq 0.8 m_G(T \sim 0).$$

b. Breit-Wigner analysis

- Above T_c, the thermal correlators deviate more and more from the single-cosh function form.

- The degrees of freedom are very different from the confinement phase.

- The scattering of strongly interacting gluons may render glueball states with thermal widths.

- Breit-Wigner ansatz:

  (N. Ishii et al, Phys. Rev. D 66, 094506 (2002))

  Thermal glueballs are treated as resonance objects which correspond to the poles, say, $\omega = \omega_0 - i\Gamma$ of the retarded and advanced Green's function in the complex $\omega -$ plane.

The spectral function is parameterized as

$$\rho(\omega) = A(\delta_\Gamma(\omega - \omega_0) - \delta_\Gamma(\omega + \omega_0) + \dots$$

$$\delta_\epsilon(x) = \frac{1}{\pi}\mathrm{Im}\left(\frac{1}{x - i\epsilon}\right) = \frac{1}{\pi}\frac{\epsilon}{x^2 + \epsilon^2}$$

As a result, the theoretical function form of the thermal correlator can be written explicitly as

$$g_\Gamma(t) = A\left[\mathrm{Re}\left(\frac{\cosh((\omega_0 + i\Gamma)(\frac{1}{2T} - t))}{\sinh(\frac{(\omega_0+i\Gamma)}{2T})}\right) + \right.$$
$$\left. 2\omega_0 T \sum_{n=1}^{\infty} \cos\left(2\pi nTt\right)\left\{\frac{1}{(2\pi nT + \Gamma)^2 + \omega_0^2} - (n \to -n)\right\}\right]$$

Which can be used to analyze the simulated correlators.

$$\left.\begin{aligned} \frac{g_\Gamma(t)}{g_\Gamma(t+1)} &= \frac{C(t,T)}{C(t+1,T)} \\ \frac{g_\Gamma(t+1)}{g_\Gamma(t+2)} &= \frac{C(t+1,T)}{C(t+2,T)} \end{aligned}\right\} \longrightarrow \omega_0(t), \Gamma(t) \longrightarrow [t_1, t_2]$$

Fit window

Taking T_2^{++} channel for instance.

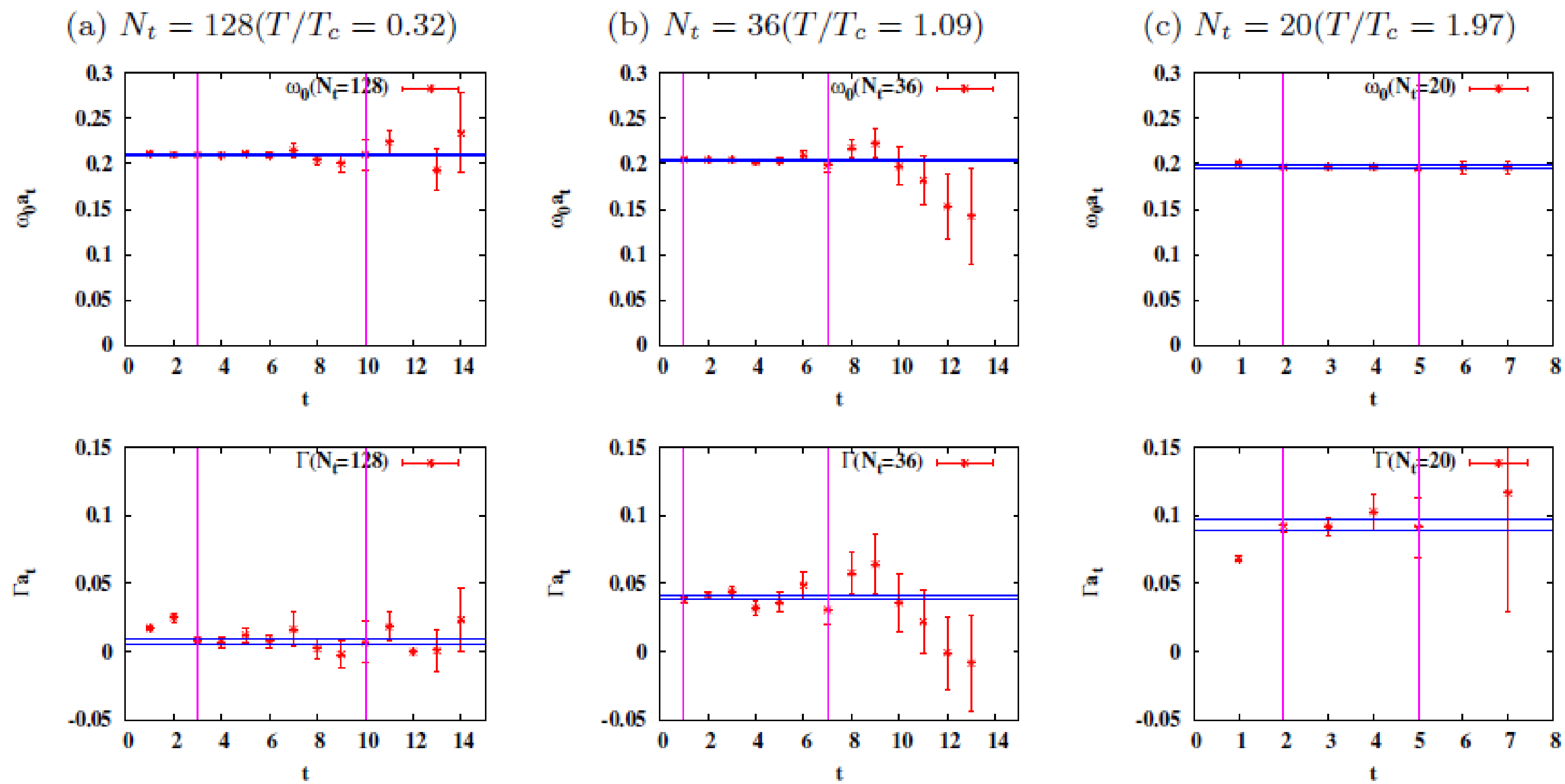

TABLE V: The best-fit ω_0 and Γ of A_1^{++} channel at different T through the Breit-Wigner fit. Also listed are the fit window $[t_1, t_2]$ and the chi-square per degree of freedom, $\chi^2/d.o.f$.

N_t	T/T_c	ω_0	Γ	$[t_1, t_2]$	$\chi^2/d.o.f$
128	0.30	0.149(1)	0.000(3)	(3, 6)	0.264
80	0.47	0.150(2)	0.005(7)	(3, 6)	0.062
60	0.63	0.152(1)	-0.001(3)	(2, 5)	0.962
48	0.79	0.158(2)	-0.010(7)	(4, 8)	1.039
44	0.86	0.155(2)	0.002(3)	(2, 4)	0.090
40	0.95	0.155(2)	-0.007(5)	(3, 7)	1.288
36	1.05	0.156(2)	0.024(2)	(1, 7)	0.496
32	1.19	0.153(2)	0.030(7)	(4,10)	0.455
28	1.36	0.154(2)	0.045(3)	(1, 7)	1.032
24	1.58	0.149(3)	0.057(3)	(1, 6)	0.472
20	1.90	0.153(4)	0.071(8)	(4, 6)	0.045

TABLE VI: The best-fit ω_0 and Γ of A_1^{-+} channel at different T through the Breit-Wigner fit. Also listed are the fit window $[t_1, t_2]$ and the chi-square per degree of freedom, $\chi^2/d.o.f$.

N_t	T/T_c	ω_0	Γ	$[t_1, t_2]$	$\chi^2/d.o.f$
128	0.30	0.226(2)	0.006(5)	(3, 9)	0.509
80	0.47	0.228(2)	0.008(4)	(2, 6)	0.640
60	0.63	0.227(1)	0.013(5)	(2, 7)	0.216
48	0.79	0.228(2)	0.012(5)	(2, 6)	0.177
44	0.86	0.229(2)	0.013(4)	(2, 8)	0.184
40	0.95	0.224(2)	0.004(6)	(3, 6)	0.549
36	1.05	0.221(2)	0.037(3)	(1, 8)	0.935
32	1.19	0.219(2)	0.047(3)	(1, 6)	0.250
28	1.36	0.211(3)	0.068(6)	(2, 5)	0.091
24	1.58	0.208(3)	0.089(7)	(2, 4)	0.003
20	1.90	0.211(3)	0.099(9)	(2, 6)	0.083

TABLE VII: The best-fit ω_0 and Γ of E^{++} channel at different T through the Breit-Wigner fit. Also listed are the fit window $[t_1, t_2]$ and the chi-square per degree of freedom, $\chi^2/d.o.f$.

N_t	T/T_c	ω_0	Γ	t_1, t_2	χ^2/DOF
128	0.30	0.212(1)	0.012(4)	(2, 5)	0.274
80	0.47	0.211(1)	0.006(3)	(2, 8)	0.616
60	0.63	0.212(1)	0.010(3)	(2, 9)	0.844
48	0.79	0.213(1)	0.011(3)	(2, 5)	0.206
44	0.86	0.211(1)	0.011(3)	(2, 8)	1.268
40	0.95	0.207(1)	0.022(3)	(2, 6)	0.250
36	1.05	0.205(2)	0.034(2)	(1, 8)	0.183
32	1.19	0.200(1)	0.049(2)	(1, 6)	0.478
28	1.36	0.191(2)	0.067(4)	(2, 6)	0.297
24	1.58	0.189(2)	0.083(5)	(2, 4)	0.253
20	1.90	0.196(2)	0.091(5)	(2, 4)	0.046

TABLE VIII: The best-fit ω_0 and Γ of T_2^{++} channel at different T through the Breit-Wigner fit. Also listed are the fit window $[t_1, t_2]$ and the chi-square per degree of freedom, $\chi^2/d.o.f$.

N_t	T/T_c	ω_0	Γ	$[t_1, t_2]$	$\chi^2/d.o.f$
128	0.30	0.210(1)	0.008(2)	(3,10)	0.442
80	0.47	0.213(1)	0.009(3)	(3, 9)	0.696
60	0.63	0.213(1)	0.012(3)	(3, 7)	0.326
48	0.79	0.210(1)	0.007(4)	(3, 6)	0.288
44	0.86	0.214(1)	0.012(2)	(2, 6)	0.437
40	0.95	0.208(1)	0.023(1)	(1, 7)	0.743
36	1.05	0.204(1)	0.039(2)	(1, 7)	0.606
32	1.19	0.199(1)	0.047(1)	(1, 6)	0.527
28	1.36	0.196(2)	0.064(3)	(2, 5)	0.022
24	1.58	0.194(1)	0.077(4)	(2, 7)	0.119
20	1.90	0.196(2)	0.093(4)	(2, 5)	0.027

The main feature of the results of Breit-Wigner analysis

- The peak positions ω_0 of the spectral functions $\rho(\omega)$ are insensitive to the temperature in all the considered channels. Especially, the ω_0 in A_1^{++} channel keeps almost constant all over the temperature range from $0.30T_c$ to $1.90T_c$. In the other three channels, the ω_0's do not change within errors below T_c, but reduce mildly with the increasing temperature above T_c. The reduction of ω_0 at the highest temperature $T = 1.90T_c$ are less than 5% in these three channels.

- In all the four channels, the thermal widths Γ are small and do not vary much below T_c, but grow rapidly with the increasing temperature when $T > T_c$. Below T_c, the thermal widths are of order $\Gamma \sim$ 5% or even smaller (especially for the A_1^{++} Γ is consistent with zero). The thermal widths increase abruptly when the temperature passes T_c and reach to values $\sim \omega_0/2$ at $T = 1.90T_c$.

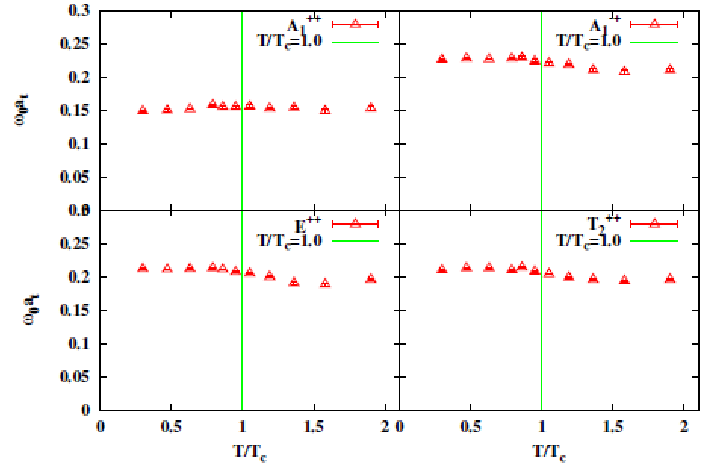

FIG. 9: ω_0's are plotted versus T/T_c for A_1^{++}, A_1^{-+} E^{++}, and T_2^{++} channels. The vertical lines indicate the critical temperature.

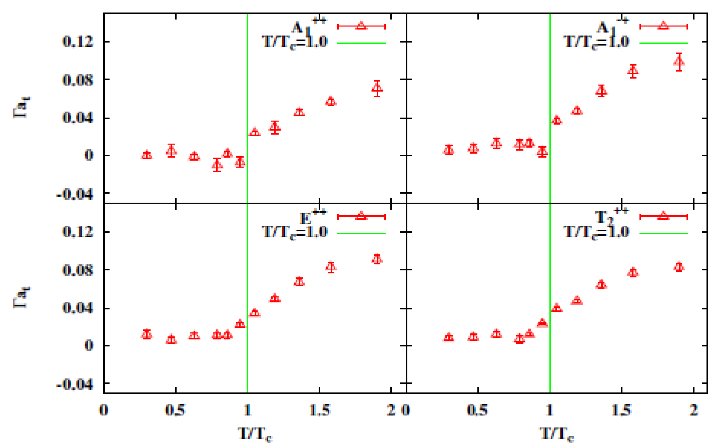

FIG. 10: Γ's are plotted versus T/T_c for A_1^{++}, A_1^{-+} E^{++}, and T_2^{++} channels. The vertical lines indicate the critical temperature.

Here we show the spectral functions based on the best fit results of ω_0 and Γ

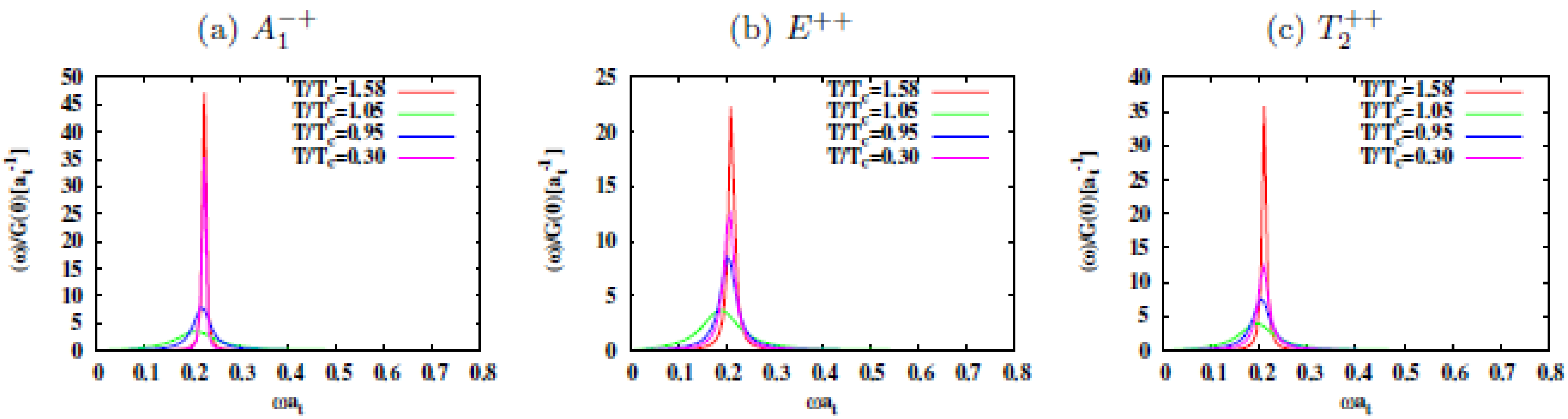

- The peak positions do not change much
- The peaks become more and more broad with the increasing of temperature.

The results of the single-cosh fit and the BW analysis are Compared in the following tables.

		A_1^{++}			A_1^{-+}		
N_t	T/T_c	m_G[GeV]	ω_0[GeV]	Γ[GeV]	m_G[GeV]	ω_0[GeV]	Γ[GeV]
128	0.30	1.689(13)	1.674(16)	-0.003(36)	2.488(31)	2.549(17)	0.069(52)
80	0.47	1.711(23)	1.689(23)	0.057(80)	2.533(24)	2.560(17)	0.086(44)
60	0.63	1.734(15)	1.714(16)	-0.012(29)	2.499(27)	2.559(16)	0.147(54)
48	0.79	1.801(20)	1.781(26)	-0.114(84)	2.533(23)	2.564(20)	0.135(55)
44	0.86	1.756(21)	1.750(17)	0.021(30)	2.454(34)	2.577(18)	0.144(48)
40	0.95	1.790(23)	1.748(20)	-0.077(52)	2.499(25)	2.525(26)	0.042(71)
36	1.05	1.621(37)	1.761(25)	0.269(26)	2.060(48)	2.490(23)	0.413(32)
32	1.19	1.486(21)	1.726(25)	0.342(81)	1.959(37)	2.464(20)	0.529(28)
28	1.36	1.418(36)	1.736(26)	0.507(28)	1.745(43)	2.375(28)	0.768(71)
24	1.58	1.351(34)	1.673(28)	0.644(33)	1.644(45)	2.308(32)	0.999(83)
20	1.90	-	1.727(42)	0.802(89)	-	2.380(35)	1.114(99)

		E^{++}			T_2^{++}		
N_t	T/T_c	m_G[GeV]	ω_0[GeV]	Γ[GeV]	m_G[GeV]	ω_0[GeV]	Γ[GeV]
128	0.30	2.364(11)	2.385(12)	0.140(42)	2.308(14)	2.363(10)	0.091(25)
80	0.47	2.308(13)	2.368(12)	0.069(29)	2.353(15)	2.387(10)	0.105(32)
60	0.63	2.330(11)	2.383(12)	0.116(32)	2.319(13)	2.396(10)	0.140(32)
48	0.79	2.353(19)	2.393(15)	0.129(34)	2.308(15)	2.362(14)	0.083(43)
44	0.86	2.319(15)	2.379(12)	0.119(32)	2.330(21)	2.405(10)	0.136(26)
40	0.95	2.263(14)	2.327(15)	0.247(38)	2.218(16)	2.344(11)	0.259(16)
36	1.05	1.880(41)	2.305(17)	0.382(23)	1.925(33)	2.298(14)	0.437(17)
32	1.19	1.722(35)	2.247(16)	0.549(20)	1.801(25)	2.244(11)	0.532(15)
28	1.36	1.610(31)	2.155(19)	0.754(43)	1.666(23)	2.205(17)	0.717(36)
24	1.58	1.565(23)	2.132(21)	0.937(55)	1.610(27)	2.184(16)	0.870(41)
20	1.90	-	2.201(23)	1.023(60)	-	2.209(20)	0.935(48)

IV. Discussions and the summary

- In the pure SU(3) gauge theory, the thermal correlators in all the 20 symmetry channels are calculated on anisotropic lattices in the temperature range from 0.3 T_c to 1.9T_c.

- Both the single-cosh fit and BW analysis show that glueballs can survive up to 1.9T_c.

- Glueball masses keep stable when the temperature increasing.

- The thermal widths of glueballs becomes larger and larger above T_c.

- It seems that in the intermediate T range, the state of matter are dominated by strongly interacting gluons. Gluons interact with each other strongly enough to form gluebal-like resonances, in the mean time, glueballs can also decay into gluons. At a given temperature, these two procedure reach the thermal equilibrium. The thermal widths signals the interaction strength.

- Our results are consistent with that of the studies of EOS and charmonia.

Dear Tony
Happy birthday

Thank You!